Damping Design for Robot Manipulators

Coleman, Tomás; Franzese, Giovanni; Borja, Pablo

DOI
10.1007/978-3-031-22731-8_6

Publication date
2023

Document Version
Final published version

Published in
Human-Friendly Robotics 2022 - HFR

Damping Design for Robot Manipulators

Tomás Coleman, Giovanni Franzese, and Pablo Borja(✉)

Department of Cognitive Robotics, Delft University of Technology, Delft, The Netherlands
{t.coleman,g.franzese}@tudelft.nl, pablo.borjarosales@plymouth.ac.uk

Abstract. This paper studies the tuning process of controllers for fully actuated manipulators. To this end, we propose a methodology to design the desired damping matrix—alternatively, the derivative gain of a PD controller—of the closed-loop system such that n second-order systems can approximate its behavior with a prescribed damping coefficient, where n denotes the degrees of freedom of the system. The proposed approach is based on the linearization of the closed-loop system around the desired configuration and is suitable for different control approaches, such as PD control plus gravity compensation, impedance control, and passivity-based control. Furthermore, we extensively analyze simulations and experimental results in a cobot.

Keywords: Damping coefficient · Performance · PD control · Impedance control

1 Introduction

Suppressing oscillations while prescribing desired stiffness values is of utmost importance in many modern robotic applications. For instance, in industrial applications, oscillations diminish the performance of robots that execute tasks involving high-speed motions [2]. Another example occurs in applications involving human-robot interaction, where robots often must be compliant enough to guarantee the safety of humans and correctly execute the task at hand [8]. Hence, choosing control gains that ensure an appropriate performance is a crucial step in designing controllers for robotic manipulators. Nevertheless, such gains are customarily selected through methods that are simple but not intuitive nor supported by an adequate analysis of the system's behavior. This ambiguity in the selection of the gains may lead to unexpected and undesirable behavior of the manipulator, which is especially important in situations where oscillations and overshoot jeopardize the success of the task. For instance, in applications involving human-robot interaction, overshoot might mean the difference between contact or no contact with the human or imply physical harm.

T. Coleman and G. Franzese: Equal contribution authorship.

P. Borja et al. (Eds.): HFR 2022, 26, pp. 74–89, 2023.
https://doi.org/10.1007/978-3-031-22731-8_6

In this paper, we propose a constructive methodology to design the damping matrix of the closed-loop system. To this end, we consider a control architecture that stabilizes the robot at the desired configuration. Then, we consider the port-Hamiltonian representation [10] of the closed-loop system and linearize it at the desired configuration. In particular, the proposed methodology is based on the simultaneous diagonalization of the inertia matrix and Hessian of the desired potential energy, yielding n second-order systems that are decoupled, where n equals the degrees of freedom of the system. Then, we design the damping coefficient for each decoupled system to prescribe the desired performance.

The proposed approach is similar to the one presented in [1]. However, two main differences with respect to the mentioned reference are:

(i) The desired potential energy is not required to be quadratic on the configuration error.
(ii) The forces Coriolis and centrifugal terms are not canceled.

The proposed approach is suitable for PD controllers, impedance control, and passivity-based controllers.

1.1 Notation

The symbol I_n denotes the $n \times n$ identity matrix; $\mathbf{0}$ is a vector or matrix whose entries are zeros; $\mathbb{1}$ is a vector whose elements equal one; $\partial f(x)/\partial x = \left[\partial f(x)/\partial x_1, \ldots, \partial f(x)/\partial x_n\right]^\top$; and $\mathtt{diag}(\cdot)$ denotes a diagonal matrix. When clear from the context, we omit the arguments of functions.

2 Proposed Methodology

2.1 Stabilization of Robotic Manipulators

A fully actuated and unconstrained robotic manipulator can be represented as follows

$$\begin{bmatrix}\dot{q}\\ \dot{p}\end{bmatrix} = \begin{bmatrix}\mathbf{0} & I_n\\ -I_n & \mathbf{0}\end{bmatrix}\begin{bmatrix}\dfrac{\partial H(q,p)}{\partial q}\\ \dfrac{\partial H(q,p)}{\partial p}\end{bmatrix} + \begin{bmatrix}\mathbf{0}\\ I_n\end{bmatrix}\tau; \quad H(q,p) := \frac{1}{2}p^\top M^{-1}(q)p + V(q), \tag{1}$$

where $q \in \mathbb{R}^n$ represents the joints configuration and $p \in \mathbb{R}^n$ the corresponding momenta; $\tau \in \mathbb{R}^m$ denotes the input vector (torques), $H : \mathbb{R}^n \times \mathbb{R}^n \to \mathbb{R}$ is the Hamiltonian (total energy) of the system; $M : \mathbb{R}^n \to \mathbb{R}^{n\times n}$ is the inertia matrix, which is positive definite; and $V : \mathbb{R}^n \to \mathbb{R}$ is the potential energy.

Theorem 1. *Consider the desired configuration $q_\star \in \mathbb{R}^n$, the desired potential energy $V_\mathtt{d} : \mathbb{R}^n \to \mathbb{R}$, and a positive definite matrix $D_\mathtt{d} \in \mathbb{R}^{n\times n}$. The control law*

$$\tau = \frac{\partial V(q)}{\partial q} - \frac{\partial V_\mathtt{d}(q)}{\partial q} - D_\mathtt{d}\dot{q} \tag{2}$$

stabilizes the system (1) *at the point* $(q_\star, \mathbf{0})$*, for any differentiable* $V_\mathtt{d}(q)$ *such that*

$$V_\mathtt{d}(q_\star) = 0 \quad \text{and} \quad V_\mathtt{d}(q) > 0, \ \forall\ q \in \mathbb{R}^n - \{q_\star\}. \tag{3}$$

Proof. From (3), we conclude that

$$H_\mathtt{d}(q_\star, \mathbf{0}) = 0 \quad \text{and} \quad H_\mathtt{d}(q,p) > 0, \ \forall\ (q,p) \in \mathbb{R}^n \times \mathbb{R}^n - \{(q_\star, \mathbf{0})\}. \tag{4}$$

Moreover, the closed-loop system takes the form

$$\begin{bmatrix} \dot{q} \\ \dot{p} \end{bmatrix} = \begin{bmatrix} \mathbf{0} & I_n \\ -I_n & -D_\mathtt{d} \end{bmatrix} \begin{bmatrix} \dfrac{\partial H_\mathtt{d}(q,p)}{\partial q} \\ \dfrac{\partial H_\mathtt{d}(q,p)}{\partial p} \end{bmatrix}; \quad H_\mathtt{d}(q,p) := \frac{1}{2} p^\top M^{-1}(q) p + V_\mathtt{d}(q). \tag{5}$$

Hence, the time derivative of $H_\mathtt{d}(q,p)$ is given by

$$\dot{H}_\mathtt{d} = \begin{bmatrix} \dfrac{\partial H_\mathtt{d}}{\partial q} \\ \dfrac{\partial H_\mathtt{d}}{\partial p} \end{bmatrix}^\top \begin{bmatrix} \mathbf{0} & I_n \\ -I_n & -D_\mathtt{d} \end{bmatrix} \begin{bmatrix} \dfrac{\partial H_\mathtt{d}}{\partial q} \\ \dfrac{\partial H_\mathtt{d}}{\partial p} \end{bmatrix} = -\left(\frac{\partial H_\mathtt{d}}{\partial p} \right)^\top D_\mathtt{d} \frac{\partial H_\mathtt{d}}{\partial p} \leq 0. \tag{6}$$

Accordingly, (4), together with (6), implies that $H_\mathtt{d}(q,p)$ qualifies as a Lyapunov function to prove the stability of the equilibrium point $(q_\star, \mathbf{0})$. For further details on Lyapunov stability, we refer the reader to [6]. Furthermore, to prove that the mentioned equilibrium is asymptotically stable—i.e., the robot converges to the desired configuration—note that

$$\dot{H}_\mathtt{d} = 0 \implies \frac{\partial H_\mathtt{d}}{\partial p} = M^{-1} p = \mathbf{0} \implies p = \mathbf{0} \implies \dot{p} = -\frac{\partial V_\mathtt{d}}{\partial q} = \mathbf{0} \implies q = q_\star.$$

Because $M^{-1}p = \dot{q}$, we conclude that $\dot{H}_\mathtt{d}$ equal to zero implies (q,p) equal to $(q_\star, \mathbf{0})$. Therefore, it follows from LaSalle's invariance principle [6] that the trajectories converge to the desired equilibrium $(q_\star, \mathbf{0})$.

□□□

Remark 1. A common choice for $V_\mathtt{d}(q)$ is

$$V_\mathtt{d}(q) = \frac{1}{2} \tilde{q}^\top K \tilde{q}, \tag{7}$$

where $K \in \mathbb{R}^{n \times n}$ is positive definite and $\tilde{q} := q - q_\star$. Moreover, the proposed selection yields

$$\tau = \frac{\partial V}{\partial q} - K\tilde{q} - D_\mathtt{d}\dot{q}, \tag{8}$$

which is a PD controller plus gravity compensation—where K is the gain of the proportional term and $D_\mathtt{d}$ corresponds to the gain of the derivative component.

Henceforth, we assume that $V_\mathtt{d}(q)$ is a twice differentiable function such that the following assumptions hold.

Assumption 1

$$\left(\frac{\partial V_{\mathtt{d}}(q)}{\partial q}\right)\Big|_{q=q_\star} = \mathbf{0} \quad \text{and} \quad \frac{\partial V_{\mathtt{d}}(q)}{\partial q} \neq \mathbf{0},\ \forall\ q \neq q_\star.$$

Assumption 2

$$\left(\frac{\partial^2 V_{\mathtt{d}}(q)}{\partial q^2}\right)\Big|_{q=q_\star} \succ 0.$$

We remark that Assumptions 1 and 2 are not necessary to prove stability. However, they are convenient to propose a constructive methodology to design $D_{\mathtt{d}}$, as shown in Sect. 2.2. Moreover, the mentioned assumptions are not restrictive from a physical point of view. Indeed, they are satisfied by (7).

2.2 Damping Design

Lemma 1. *Consider two positive definite matrices, namely, $N, P \in \mathbb{R}^{n\times n}$. There exists an invertible matrix $W \in \mathbb{R}^{n\times n}$ such that*

$$W^\top N W = I_n \quad \text{and} \quad W^\top P W = \Sigma,$$

where $\Sigma \in \mathbb{R}^{n\times n}$ is a diagonal matrix such that the elements of its main diagonal are positive.

Proof. Because N is positive definite, its inverse exists and is positive definite. Hence, there exists a full rank matrix $\phi_{\mathtt{n}} \in \mathbb{R}^{n\times n}$ such that $N^{-1} = \phi_{\mathtt{n}}^\top \phi_{\mathtt{n}}$.[1] Moreover, the matrix $\phi_{\mathtt{n}} P \phi_{\mathtt{n}}^\top$ is positive definite. Thus, its singular value decomposition (SVD) yields

$$\phi_{\mathtt{n}} P \phi_{\mathtt{n}}^\top = U \Sigma U^\top,$$

where $U \in \mathbb{R}^{n\times n}$ is an orthogonal matrix, i.e., $U^\top = U^{-1}$. Select $W = \phi_{\mathtt{n}}^\top U$. Then, the proof is completed noting that

$$\begin{aligned} W^\top N W &= U^\top \phi_{\mathtt{n}} \phi_{\mathtt{n}}^{-1} \phi_{\mathtt{n}}^{-\top} \phi_{\mathtt{n}}^\top U = U^\top U = I_n; \\ W^\top P W &= U^\top \phi_{\mathtt{n}} P \phi_{\mathtt{n}}^\top U = U^\top U \Sigma U^\top U = \Sigma. \end{aligned}$$

□□□

To simplify the notation, we introduce the following matrix

$$\mathcal{K} := \left(\frac{\partial^2 V_{\mathtt{d}}}{\partial q^2}\right)\Big|_{q=q_\star}.$$

Moreover, we consider the full rank matrix $\phi_{\mathtt{m}} \in \mathbb{R}^{n\times n}$ such that

$$M^{-1}(q_\star) = \phi_{\mathtt{m}}^\top \phi_{\mathtt{m}}. \tag{9}$$

[1] The matrix $\phi_{\mathtt{n}}$ can be obtained via Cholesky decomposition or singular value decomposition. For further details, we refer the reader to [5].

Accordingly, the SVD of $\phi_{\mathtt{m}}\mathcal{K}\phi_{\mathtt{m}}^{\top}$ is given by

$$\phi_{\mathtt{m}}\mathcal{K}\phi_{\mathtt{m}}^{\top} = U_{\mathtt{mk}}\Sigma_{\mathtt{mk}}U_{\mathtt{mk}}^{\top}, \tag{10}$$

where $U_{\mathtt{mk}} \in \mathbb{R}^{n\times n}$ is an orthogonal matrix and

$$\Sigma_{\mathtt{mk}} := \mathtt{diag}(\sigma_{\mathtt{mk}_1}, \ldots, \sigma_{\mathtt{mk}_n}) \succ 0. \tag{11}$$

Proposition 1. Consider the system (5) and the desired configuration $q_\star$, such that $V_{\mathtt{d}}(q)$ satisfies Assumptions 1 and 2. There exist $W_{\mathtt{mk}} \in \mathbb{R}^{n\times n}$, full rank, and $\Sigma_{\mathtt{D}} \in \mathbb{R}^{n\times n}$, diagonal positive definite, such that the selection

$$D_{\mathtt{d}} = W_{\mathtt{mk}}^{-\top}\Sigma_{\mathtt{D}}W_{\mathtt{mk}}^{-1} \tag{12}$$

ensures that the trajectories of (5) behave as the response of n second-order systems as they approach the equilibrium. Moreover, the damping coefficients of such second-order systems are determined by

$$\xi_i = \frac{\sigma_{\mathtt{D}_i}}{2\sqrt{\sigma_{\mathtt{mk}_i}}}, \qquad i \in \{1, \ldots, n\}, \tag{13}$$

where $\sigma_{\mathtt{D}_i}$ and $\sigma_{\mathtt{mk}_i}$ correspond to the main diagonal elements of $\Sigma_{\mathtt{mk}}$, defined in (11), and $\Sigma_{\mathtt{D}}$, respectively.

Proof. Define $M_\star := M(q_\star)$. Then, the linearization of (5) around the point $(q_\star, \mathbf{0})$ is given by $\dot{z} = \mathcal{A}z$, where

$$z := \begin{bmatrix} q - q_\star \\ p \end{bmatrix}, \quad \mathcal{A} := \begin{bmatrix} \mathbf{0} & M_\star^{-1} \\ -\mathcal{K} & -D_{\mathtt{d}}M_\star^{-1} \end{bmatrix}. \tag{14}$$

Consider the matrices

$$S_{\mathtt{d}} := \begin{bmatrix} I_n & \mathbf{0} \\ \mathbf{0} & M_\star^{-1} \end{bmatrix}, \quad \mathcal{A}_{\mathtt{d}} := \begin{bmatrix} \mathbf{0} & I_n \\ -M_\star^{-1}\mathcal{K} & -M_\star^{-1}D_{\mathtt{d}} \end{bmatrix}.$$

Note that $\mathcal{A}_{\mathtt{d}} = S_{\mathtt{d}}\mathcal{A}S_{\mathtt{d}}^{-1}$. Thus, $\mathcal{A}_{\mathtt{d}}$ is similar to $\mathcal{A}$, consequently their eigenvalues are the same. Furthermore, $\mathcal{A}_{\mathtt{d}}$ is a companion matrix of

$$L(\lambda) = I_n\lambda^2 + M_\star^{-1}D_{\mathtt{d}}\lambda + M_\star^{-1}\mathcal{K}.$$

Hence, the eigenvalues of $\mathcal{A}_{\mathtt{d}}$ are determined by the values $\lambda \in \mathbb{C}$ such that $L(\lambda)$ loses rank, i.e., its determinant equals zero [7]. Since $M_\star$ is full rank, we have the following chain of implications

$$\det(L) = 0 \iff \det(M_\star^{-1})\det(M_\star L) = 0 \iff \det\left(M_\star\lambda^2 + D_{\mathtt{d}}\lambda + \mathcal{K}\right) = 0. \tag{15}$$

Moreover, invoking the result of Lemma 1, there exists a full rank matrix $W_{\mathtt{mk}} \in \mathbb{R}^{n\times n}$ such that

$$W_{\mathtt{mk}}^{\top}\left(M_\star\lambda^2 + D_{\mathtt{d}}\lambda + \mathcal{K}\right)W_{\mathtt{mk}} = I_n\lambda^2 + W_{\mathtt{mk}}^{\top}D_{\mathtt{d}}W_{\mathtt{mk}}\lambda + \bar{\Sigma},$$

where $\bar{\Sigma}$ is a diagonal positive definite matrix. Hence, by choosing $D_{\mathtt{d}}$ as in (12), we obtain

$$\det(L) = 0 \iff \det\left(I_n\lambda^2 + \Sigma_{\mathtt{D}}\lambda + \bar{\Sigma}\right) = 0. \tag{16}$$

Note that $I_n\lambda^2 + \Sigma_{\mathtt{D}}\lambda + \bar{\Sigma}$ is a diagonal matrix. Hence, its determinant is zero if and only if one of its main diagonal elements equals zero. Consequently, (16) can be analyzed as n decoupled second-order systems. Furthermore, following the rationale in the proof of Lemma 1, we get that

$$W_{\mathtt{mk}} = \phi_{\mathtt{mk}}^{\top} U_{\mathtt{mk}} \quad \text{and} \quad \bar{\Sigma} = \Sigma_{\mathtt{mk}} \tag{17}$$

with $\phi_{\mathtt{m}}^{\top}$, $U_{\mathtt{mk}}$, and $\Sigma_{\mathtt{mk}}$ defined as in (9), (10), and (11), respectively. Therefore, the n second-order equations take the form

$$\lambda^2 + \sigma_{\mathtt{D}_i}\lambda + \sigma_{\mathtt{mk}_i} = 0. \tag{18}$$

Hence, equating (18) with the standard structure of a second-order system, i.e.,

$$\lambda^2 + 2\xi_i\omega_{\mathtt{n}_i}\lambda + \omega_{\mathtt{n}_i}^2 = 0,$$

we obtain (13). □□□

Remark 2. The model (1) is valid—considering appropriate coordinates—for the joint and task spaces. Consequently, the result of Proposition 1 is suitable to design the damping matrix in both spaces.

The proposed approach assumes that the stiffness matrix K is fixed for the specific purposes of the application at hand, i.e., the method is devised to compute $D_{\mathtt{d}}$ for a given K. However, the performance of the closed-loop system can be enhanced if K and $D_{\mathtt{d}}$ can be designed simultaneously. We illustrate this in Sect. 3.1.

Table 1. Different simulation cases

Case	C1	C2	C3	C4	C5	C6	C7	C8	C9	C10	C11
$q_\star$	$\frac{\mathbb{1}}{4}$	$\frac{\mathbb{1}}{4}$	$\frac{\mathbb{1}}{4}$	$\frac{\mathbb{1}}{4}$	$\frac{\mathbb{1}}{4}$	$\frac{\mathbb{1}}{2}$	$\frac{\mathbb{1}}{10}$	$\frac{\mathbb{1}}{4}$	$\frac{\mathbb{1}}{4}$	$\frac{\mathbb{1}}{4}$	$\frac{\mathbb{1}}{4}$
ξ	1	$\frac{\sqrt{2}}{2}$	1.5	$\xi_{\mathtt{d}}$	1	1	1	1	1	1	1
K	$K_{\mathtt{d}}$	$K_{\mathtt{d}}$	$K_{\mathtt{n}}$	$K_{\mathtt{d}}$	$K_{\mathtt{n}}$	$K_{\mathtt{d}}$	$K_{\mathtt{d}}$	$K_{\mathtt{m}}$	$\frac{K_{\mathtt{d}}}{4}$	$\frac{K_{\mathtt{d}}}{4}$	–

3 Results

We design the damping matrix of a *Franka Emika Panda* robot in joint space to validate the methodology. This robot has seven degrees of freedom given by the angles of seven revolute joints, denoted as q_i, with $i \in \{1, \ldots, 7\}$. We simulate the behavior of the closed-loop system considering different scenarios. Then, we perform two experiments: (i) we implement the proposed methodology to design $D_{\mathtt{d}}$, and (ii) we implement the controller provided in https://github.com/franzesegiovanni/franka_human_friendly_controllers.

3.1 Simulations

We consider the open-loop dynamics provided in [4].[2] Then, we simulate eleven different cases given in Table 1, where

$$\xi_{\mathtt{d}} = \begin{bmatrix} 0.5 & 0.7 & 0.7 & 1 & 1.3 & 1.3 & 1.5 \end{bmatrix}; \qquad K_{\mathtt{d}} = \mathtt{diag}(80, 40, 80, 40, 80, 80, 20);$$
$$K_{\mathtt{m}} = 1000\phi_{\mathtt{m}}^{-1}\mathtt{diag}(2.5, 2.5, 2.5, 2.5, 3.6, 2.5, 10)\phi_{\mathtt{m}}^{-\top};$$

$$K_{\mathtt{n}} = \begin{bmatrix} 80 & 0 & 0 & 0 & 0 & 0 & 0 \\ 0 & 184 & 0 & -72 & 0 & 0 & 0 \\ 0 & 0 & 80 & 0 & 0 & 0 & 0 \\ 0 & -72 & 0 & 76 & 0 & 0 & 0 \\ 0 & 0 & 0 & 0 & 80 & 0 & 0 \\ 0 & 0 & 0 & 0 & 0 & 80 & 0 \\ 0 & 0 & 0 & 0 & 0 & 0 & 20 \end{bmatrix}.$$

For simulation purposes, we consider initial conditions $q_0 = \mathbf{0}$ in all the cases. Moreover, in all the cases—except for **C4**—we consider the same damping coefficient for the seven second-order equations (13).

For all the considered scenarios—except for **C10**—we compute $D_{\mathtt{d}}$ via the approach proposed in Sect. 2.2. In contrast to the rest of cases, in **C10** we consider $M(q_\star) = I_7$ to design $D_{\mathtt{d}}$. Hence, (13) can be rewritten as $\sigma_{\mathtt{d}_i} = 2\xi_i\sqrt{k_i}$ for $i \in \{1, \ldots, 7\}$. Thus, recalling that al the damping coefficients ξ_i are the same and K is a diagonal matrix[3] in **C10**, we have

$$D_{\mathtt{d}} = 2\xi K^{\frac{1}{2}}. \tag{19}$$

The expression (19) is common in practice to design $D_{\mathtt{d}}$. However, this approach is suitable only for diagonal stiffness matrices and completely neglects the inertia matrix of the system, which is one of the main sources of the nonlinear behavior of a robot. Henceforth, we refer to the expression (19) as the *naive approach* to design $D_{\mathtt{d}}$.

In all the cases—except for **C11**—we consider a control law of the form (8). Depending on the source, this control approach can be understood as a PD controller plus gravity compensation, an impedance control, or a particular class of passivity-based control strategy. For **C11**, we consider the control law (2) and the desired potential energy

$$V_{\mathtt{d}} = \sum_{i=1}^{7} \alpha_i \ln\left(\cosh(10\tilde{q}_i)\right) + \frac{1}{4}\tilde{q}_2^4,$$

[2] See https://github.com/marcocognetti/FrankaEmikaPandaDynModel.
[3] Namely, $K = \frac{1}{4}K_{\mathtt{d}}$.

with $\alpha_1 = \alpha_3 = \alpha_5 = \alpha_6 = 0.8$, $\alpha_2 = \alpha_4 = 0.4$, and $\alpha_7 = 0.2$. Thus,

$$\frac{\partial V_{\mathtt{d}}(q)}{\partial q} = \begin{bmatrix} 8\tanh(10\tilde{q}_1) \\ 4\tanh(10\tilde{q}_2) + \tilde{q}_2^3 \\ 8\tanh(10\tilde{q}_3) \\ 4\tanh(10\tilde{q}_4) \\ 8\tanh(10\tilde{q}_5) \\ 8\tanh(10\tilde{q}_6) \\ 2\tanh(10\tilde{q}_7) \end{bmatrix}.$$

We stress that the concept of stiffness matrix in impedance control is not valid for this case. Consequently, approaches as the one proposed in [1] are not suitable for this control law. Nevertheless, the method to design $D_{\mathtt{d}}$ proposed in Sect. 2.2 is still valid. Furthermore, the linearized systems obtained from **C1** and **C11** are the same.

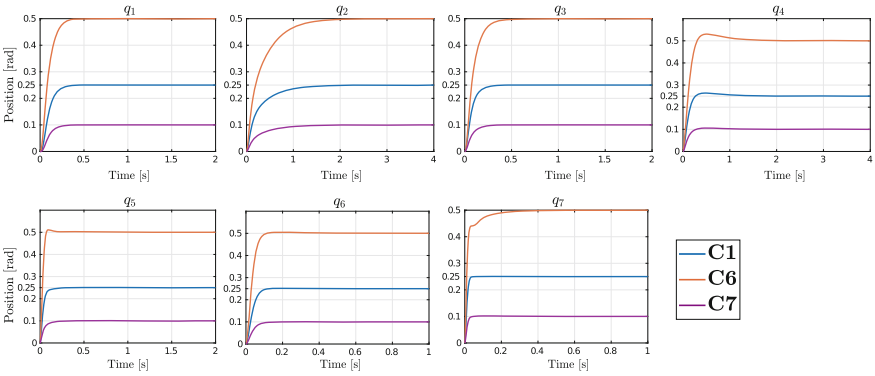

Fig. 1. Trajectories of the joints for a critically damped design and different references.

Limitations Due to Linearization The robotic manipulator used for simulations and experiments is a nonlinear system, while the proposed methodology to design $D_{\mathtt{d}}$ relies on linearizing the closed-loop system. Therefore, the performance analysis, i.e., the assignation of ξ, is valid only in a region close to the desired configuration. However, we underscore that the asymptotic stability of the desired equilibrium is guaranteed for the nonlinear model, i.e., the robot converges to the desired configuration independently of the validity of the linearized system using to design $D_{\mathtt{d}}$. Unfortunately, the closed-loop system may exhibit different performance than the desired one for initial conditions far from the desired configuration. Nonetheless, in practice, the proposed method is expected to yield reasonable good behavior.

Figure 1 shows the plots of **C1**, **C6**, and **C7**. In these three cases $D_{\mathtt{d}}$ is desgined such that the seven second-order systems are critically damped. Thus,

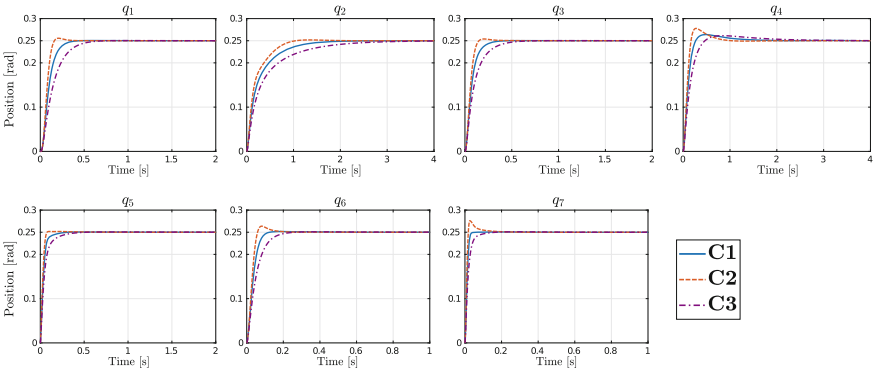

Fig. 2. Trajectories of the joints for different damping coefficients.

the trajectories of the joints should not exhibit overshoot. We observe in the simulations that the result is more accurate for a reference that is closer to the initial conditions—see the plots corresponding to **C6**. However, in **C1** and **C7**, we note overshoot in some of the joints—particularly q_4—as the reference is set farther from the initial conditions.

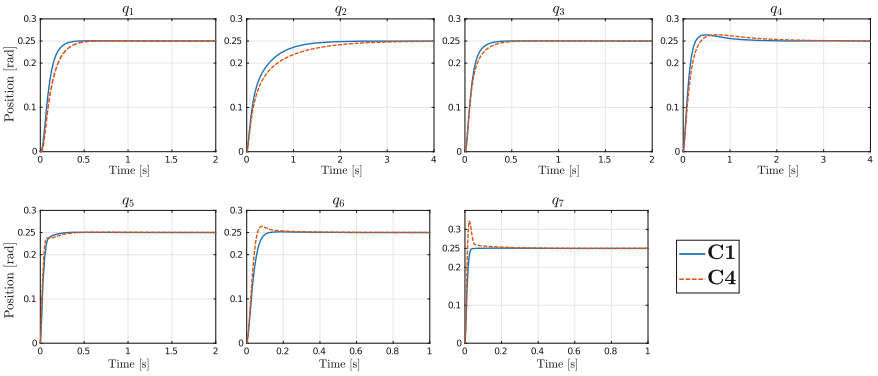

Fig. 3. Comparison between **C1** and **C4**. The damping coefficients ξ_i are designed independently in the latter case.

Choosing $\boldsymbol{\xi}$. The proposed approach permits assigning different damping coefficients to the seven second-order systems, which can be exploited to mitigate overshoot in their responses or increase convergence speed. In particular, we expect a faster convergence for $\xi < 1$ at expenses of some overshoot. Moreover, we expect that the response for $\xi > 1$ convegence slower than the one for $\xi = 1$. Figure 2 depicts the plots of **C1**, **C2**, and **C3**, where only ξ is modified. We observe that the convergence rates behave as predicted. However, in **C1**, which corresponds to seven critically damped systems, q_2 and q_5 behave as overdamped

systems, while we appreciate overshoot in q_4—i.e., it behaves as an underdamped system.

While it is possible to design the damping coefficients independently, the intuition to propose them properly is not straightforward because the method changes the basis of the system—through the linear transformation $W_{\mathtt{mk}}$—to obtain the seven second-order systems. To illustrate this, in **C4**, we propose damping coefficients such that we could suppose three overdamped responses, three underdamped responses, and one critically damped response. Figure 3 shows the plots of **C1** and **C4**. For the latter, there is no critically damped response. Moreover, it is unclear how the proposed damping coefficients affect the response of each joint.

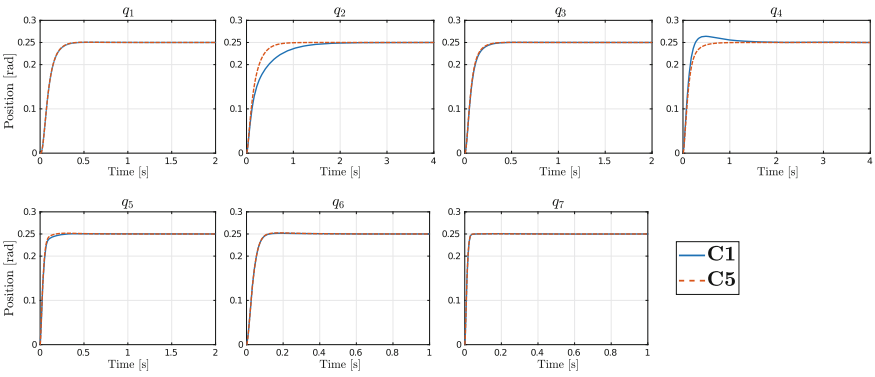

Fig. 4. Comparison between **C1** and **C5**, where the latter considers a non-diagonal stiffness matrix.

Non-diagonal K**.** In practice, the stiffness matrix is often proposed diagonal for simplicity—for instance [3]. Nevertheless, this approach is not convenient in some applications involving human-robot interaction, e.g., [9]. Moreover, the behavior of the joints is physically coupled. This coupling is the result of the non-diagonal structure of the mass inertia matrix. Hence, choosing K diagonal might not be physically intuitive.

Note that the simulations of **C1** show unexpected behaviors for q_2 and q_4. Whence, we can conjecture that the nonlinearities (physical couplings) have a greater impact on these coordinates than in the rest. To address this issue, in **C5**, we propose a stiffness matrix—namely, $K_{\mathtt{n}}$—that couples q_2 and q_4. Then, in both cases, the damping matrix is obtained via the approach proposed in Sect. 2.2. Figure 4 shows the comparison between **C1** and **C5**, where the latter performs better than the former—especially for q_2 and q_4. While the design of the stiffness matrix is based on the system's physics, it does not stem from a formal argument, and further research on this topic is necessary.

If K is free, then the design of $D_{\mathtt{d}}$ can be simplified by choosing K based on $M(q_\star)$. In particular, the selection

$$K = \phi_{\mathtt{m}}^{-1} \Sigma_{\mathtt{K}} \phi_{\mathtt{m}}^{-\top}; \quad \Sigma_{\mathtt{K}} := \mathtt{diag}(\sigma_{\mathtt{K}_1}, \ldots, \sigma_{\mathtt{K}_n}) \succ 0$$

yields $W_{\mathtt{mk}} = \phi_{\mathtt{m}}^{\top}$ in (12). Hence, (13) reduces to

$$\xi_i = \frac{\sigma_{\mathtt{D}_i}}{2\sqrt{\sigma_{\mathtt{K}_i}}}, \qquad i \in \{1, \ldots, n\},$$

which is similar to the naive approach. Figure 5 depicts the comparison between **C1** and **C8**, where the stiffness matrix is proposed based on $M(q_\star)$. In the mentioned figure, we observe that the trajectories of all the joints, except for q_7, exhibit a better performance when the K is based on the inertia matrix.

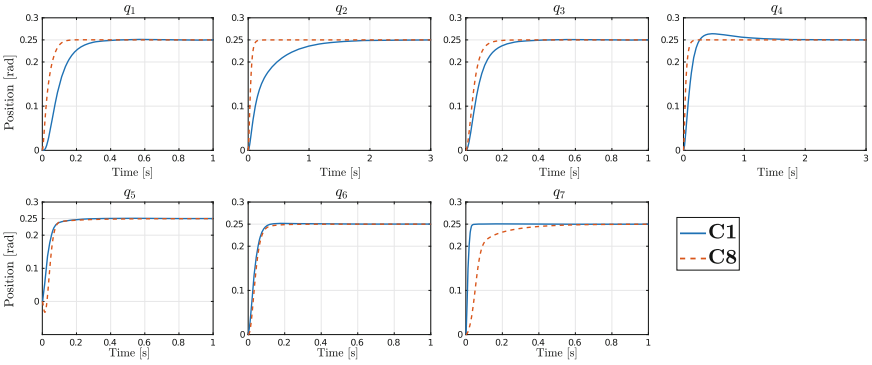

Fig. 5. Comparison between **C1** and **C8**, where the latter considers a stiffness matrix based on the inertia matrix of the system.

Proposed Method vs Naive Approach. The controllers designed by adopting the naive approach are suitable to stabilize the robot at its desired configuration because they satisfy the conditions provided in Sect. 2.1, i.e., the point $(q_\star, \mathbf{0})$ is a globally asymtotically equilibrium for the closed-loop system. An advantage of this method is its simplicity. On the other hand, an important disadvantage is the lack of intuition into how to prescribe a desired performance for the closed-loop system. Figure 6 illustrates the comparison between the damping design method proposed in Sect. 2.2 (**C9**) and the naive approach (**C10**) under the same conditions, where we observe that the proposed methodology outperforms the naive approach except for joints 2 and 4.

Linear vs Nonlinear Proportional Term. Some applications require desired potential energies that are not quadratic on the position error, e.g., [11]. Consequently, the gradient of the $V_{\mathtt{d}}(q)$ is nonlinear and the closed-loop system has no

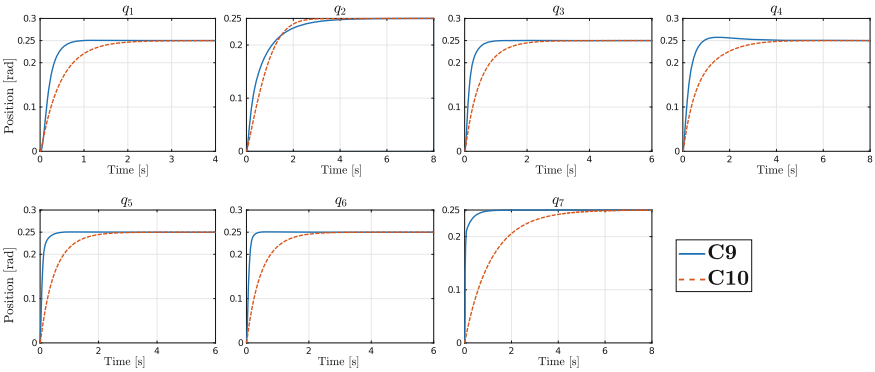

Fig. 6. Comparison between the proposed methodology (**C9**) and the naive approach (**C10**).

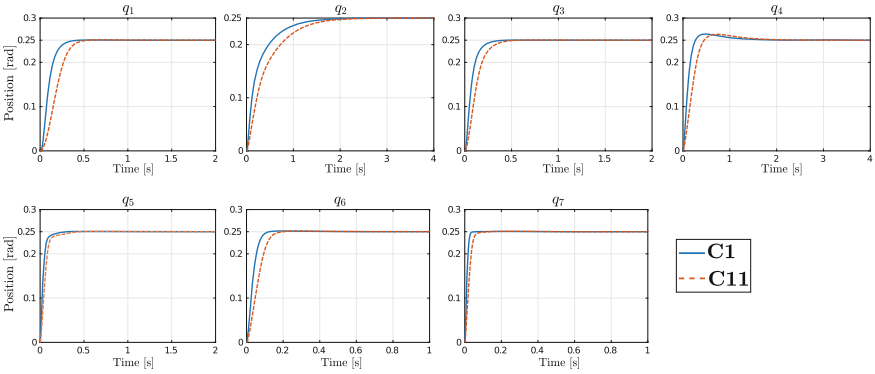

Fig. 7. Trajectories of a closed-loop system whose potential energy is quadratic on the position error (**C1**) and a closed-loop system whose potential energy is non quadratic on the position error (**C11**).

stiffness matrix. Nevertheless, since the proposed methodology is based on the linearization, it is still suitable to design the damping matrix for the closed-loop system. Figure 7 shows the trajectories of two systems whose linearizations are identical. However, one case considers a quadratic potential energy (**C1**) and the other corresponds to a non quadratic $V_{\mathtt{d}}(q)$ (**C11**).

3.2 Experimental Results

The procedure to validate the proposed methodology consists in calculating the damping matrix for for the closed-loop system (5) for a given desired potential energy of the form (7).[4] Then, we simultaneously change the desired angle of all

[4] The code to implement the proposed controller in the Panda robot is available at https://github.com/franzesegiovanni/franka_damping_design.

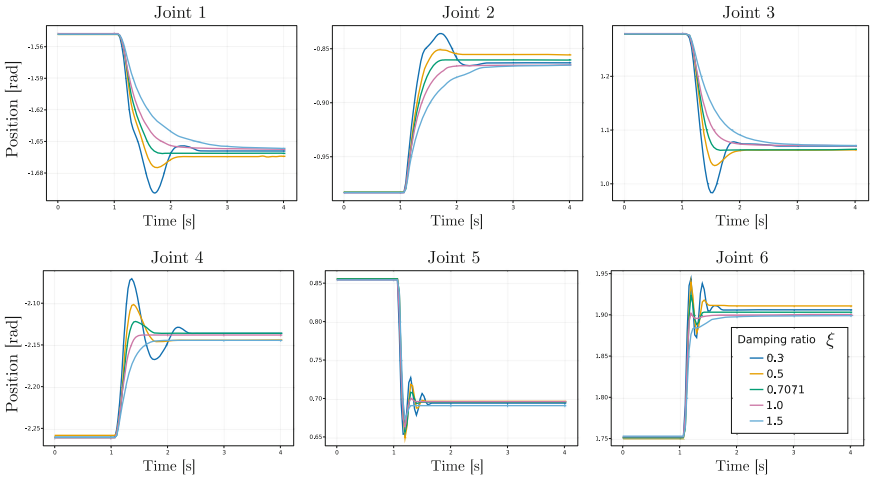

Fig. 8. Trajectory of each joint of the robot, for a reference of 0.1 rad from q_0, using the proposed damping design method. The damping matrix is updated at a frequency of 1 kHz at the current position.

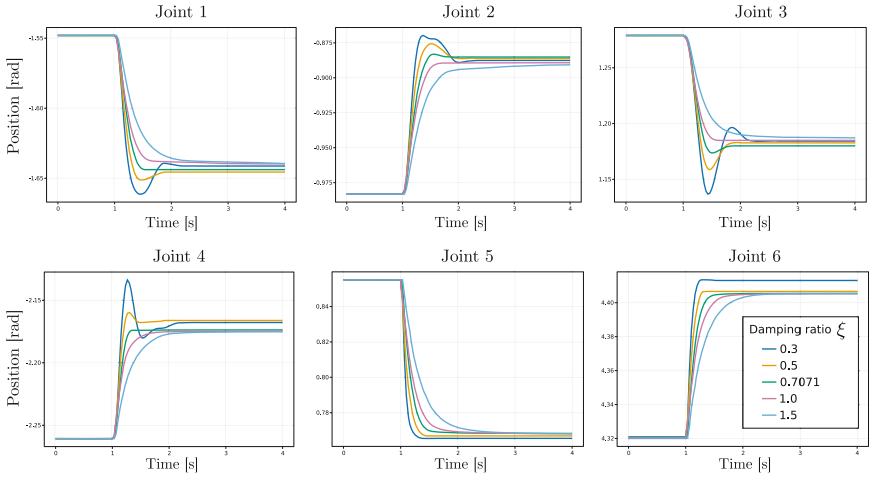

Fig. 9. Trajectory of each joint of the robot, for a reference of 0.1 rad from q_0, using the naive approach.

joints of the *Franka Emika Panda* robot. The initial configuration of the robot is given by

$$q_0 = \begin{bmatrix} -1.548 & -0.9832 & 1.2789 & -2.2607 & 0.8551 & 1.7509 & 0.1978 \end{bmatrix}^\top .$$

Moreover, the stiffness matrix considered for the experiments is given by

$$K = \texttt{diag}(100, 100, 100, 100, 100, 100, 8)$$

and the mass matrix is obtained using the functionality in the *Franka Emika Panda's* controller code base 'franka_ros'.[5]

The results in Fig. 8 show that, by adopting the proposed methodology, the variations in ξ_i affect the characteristic response of the system as expected, i.e., the system overshoots and oscillates more when the damping ratio decreases and when the damping ratio increases above $\xi_1 = 1$, the convergence is slower. We also observe that the steady-state error is affected by the selection of ξ. In particular, we omit the plot of q_7 because the response is too sensitive to provide a meaningful comparison.

The results of the same experiments, but carried out with naive approach, are shown in Fig. 9. It can be seen that the effect of selecting a specific damping ratio does not affect the performance in the expected manner in all the joints. This is especially apparent in the joints 4, 5, and 6 where even for low damping ratios, the system is drastically over damped. This highlights a major problem for the designer, as there is no correlation between the damping ratios and the characteristic behaviour of the joints. In this experiment, the joints 2 and 3 perform as expected, where the trajectories are underdamped, critically damped, and overdamped for $\xi = 0.7071$, $\xi = 1$, and $\xi = 1.5$, respectively. The mentioned behavior changes according to the robot's configuration, leading to the conclusion that the good performance at particular joints is because the assumption $M(q_\star) = I_7$ is an adequate approximation in that particular position and not by design.

The inconsistency of the naive approach is further highlighted in Fig. 10. Here, it can be more clearly seen that, using both methods, the joint is critically damped for $\xi = 1$. However, for $\xi = \sqrt{2}/2$, the response is underdamped (as expected) for the proposed methodology, while for the naive approach is still critically damped. Moreover, the naive approach results in a larger steady-state error for both damping ratios.

4 Conclusions

We have provided a method to design the damping matrix for fully actuated robotic arms, which is based on the linearization of the system and fits in different approaches, such as PD control, impedance control, and passivity-based control.

[5] See https://github.com/frankaemika/franka_ros.

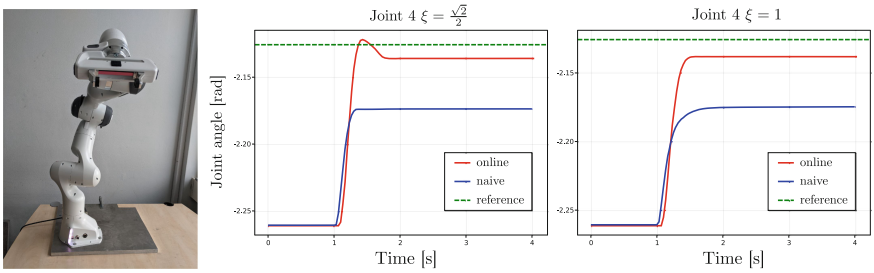

Fig. 10. Panda robot used for the experiments (left). Comparison of the trajectories of Joint 4 with $\xi = \sqrt{2}/2$ and $\xi = 1$ (right). Here, the plot corresponding to the proposed method is labeled as *online*.

We have shown that the proposed method is more consistent than the naive approach, which neglects the physical coupling given by the inertia matrix of the system. Moreover, we have provided some intuitive alternatives to design the stiffness matrix to enhance the performance of the closed-loop system. Finally, we have performed simulations and experiments to validate the methodology, supporting the theoretical claims.

Acknowledgments. The authors thank Cosimo Della Santina for the fruitful discussions during the elaboration of this manuscript.

Tomás Coleman's research is funded by the Netherlands Organization for Scientific Research project Cognitive Robots for Flexible Agro-Food Technology, grant P17-01.

Giovanni Franzese's research is funded by the European Research Council Starting Grant Teaching Robots Interactively (TERI), project reference 804907.

References

1. Albu-Schäffer, A., et al.: Cartesian impedance control of redundant robots: recent results with the DLR-light-weight-arms. In: 2003 IEEE International Conference on Robotics and Automation, vol. 3, pp. 3704–3709 (2003)
2. Albu-Schäffer, A., et al.: The DLR lightweight robot: design and control concepts for robots in human environments. Ind. Robot: Int. J. (2007)
3. Franzese, G., et al.: ILoSA: interactive learning of stiffness and attractors. In: 2021 IEEE/RSJ International Conference on Intelligent Robots and Systems (IROS), pp. 7778–7785. IEEE (2021)
4. Gaz, C., et al.: Dynamic identification of the Franka Emika panda robot with retrieval of feasible parameters using penalty-based optimization. IEEE Robot. Autom. Lett. **4**(4), 4147–4154 (2019)
5. Horn, R.A., Johnson, C.R.: Matrix Analysis. Cambridge University Press (2012)
6. Khalil, H.K.: Nonlinear Systems, 3rd edn. Prentice-Hall, New Jersey (2002)
7. Marcus, M., Minc, H.: A Survey of Matrix Theory and Matrix Inequalities, vol. 14. Courier Corporation (1992)
8. Peternel, L., et al.: Teaching robots to cooperate with humans in dynamic manipulation tasks based on multi-modal human-in-the-loop approach. Autonomous Robot. **36**(1), 123–136 (2014)

9. Prendergast, J.M., et al.: Biomechanics aware collaborative robot system for delivery of safe physical therapy in shoulder rehabilitation. IEEE Robot. Autom. Lett. **6**(4), 7177–7184 (2021)
10. van der Schaft, A.J., Jeltsema, D.: Port-Hamiltonian systems theory: an introductory overview. Foundations Trends Syst. Control **1**(2–3), 173–378 (2014)
11. Wesselink, T.C., Borja, P., Scherpen, J.M.A.: Saturated control without velocity measurements for planar robots with flexible joints. In: 2019 IEEE 58th Conference on Decision and Control (CDC), pp. 7093–7098. IEEE (2019)